

Document downloaded from:

<http://hdl.handle.net/10251/189495>

This paper must be cited as:

Sánchez-Arévalo, CM.; Jimeno-Jiménez, Á.; Carbonell Alcaina, C.; Vincent Vela, MC.; Alvarez Blanco, S. (2021). Effect of the operating conditions on a nanofiltration process to separate low-molecular-weight phenolic compounds from the sugars present in olive mill wastewaters. *Process Safety and Environmental Protection*. 148:428-436.  
<https://doi.org/10.1016/j.psep.2020.10.002>



The final publication is available at

<https://doi.org/10.1016/j.psep.2020.10.002>

Copyright Elsevier

Additional Information

1  
2  
3  
4  
5  
6  
7  
8  
9  
10  
11  
12  
13  
14  
15  
16  
17  
18  
19  
20  
21  
22  
23  
24  
25  
26  
27  
28  
29

**Effect of the operating conditions on a nanofiltration process to separate low-molecular-weight phenolic compounds from the sugars present in olive mill wastewaters**

Carmen M. Sánchez-Arévalo,<sup>1</sup> Álvaro Jimeno-Jiménez<sup>1</sup>, Carlos Carbonell-Alcaina<sup>1,2</sup>, María Cinta Vincent-Vela,<sup>1,2</sup> Silvia Álvarez-Blanco<sup>1,2</sup>.

<sup>1</sup>Research Institute for Industrial, Radiophysical and Environmental Safety (ISIRYM), Universitat Politècnica de València, Camino de Vera, s/n, 46022, Valencia, Spain.

<sup>2</sup>Department of Chemical and Nuclear Engineering, Universitat Politècnica de València, C/Camino de Vera s/n, 46022 Valencia, Spain

\*Corresponding author: S. Álvarez-Blanco<sup>1</sup>

**E-mail:** sialvare@iqn.upv.es

30 **Abstract**

31 The efficiency of nanofiltration to purify the tyrosol present in the olive mill wastewaters  
32 (OMWWs) has been studied. The similar molecular weight of tyrosol and the sucrose existing in  
33 this kind of by-products restricts the discrimination between both molecules through a  
34 membrane process, but the interest of phenolic compounds to be applied in cosmetics and  
35 pharmacology greatly motivates its recovery at the highest purity possible. Thus, two different  
36 simulated OMWWs composed of tyrosol and mixtures of tyrosol and sucrose, respectively, were  
37 nanofiltered using the NF270 membrane. Three transmembrane pressures (TMPs) and three  
38 cross-flow velocities were tested. The optimum results were obtained at  $0.5 \text{ m}\cdot\text{s}^{-1}$  and 15 bar.  
39 The rejections of the chemical oxygen demand (COD) were above 78%, whereas phenolic  
40 compounds were barely retained. This indicates that the sugar was accurately separated from  
41 tyrosol, which was recovered in the permeate stream at a high purity.

42

43 **Keywords:** nanofiltration; olive mill wastewater; phenolic compounds; sucrose; separation.

44

## 45 Introduction

46 For some years now, phenolic compounds from the olive fruit have called particular attention.  
47 Apart from being responsible for the sensorial characteristics and stability of virgin olive oil, their  
48 principal meaning relies on their antioxidant and anti-inflammatory properties, that have been  
49 widely related with potential health benefits, including preventing the risk of suffering some  
50 heart and neurological diseases and even cancer. As a consequence of these outstanding  
51 properties, food, pharmaceutical and cosmetic industries have shown a great interest in these  
52 compounds (Casaburi et al., 2013; Ghanbari et al., 2012; López-Miranda et al., 2010; Ray et al.,  
53 2019).

54 Phenolic compounds are present in every product derived from the olive grove, including olive  
55 leaves, stems, seeds, fruit skin, fruit pulp and obviously olive oil (Olmo-García et al., 2018). As a  
56 result, these molecules can be found in the residues obtained after olive processing too. A  
57 considerable percentage of the phenolic compounds of the olive drupe is transferred to the  
58 wastewaters obtained in the olive mills (olive mill wastewaters<sup>1</sup>, OMWWs) (Di Mauro et al.,  
59 2017), and they are also present in the brines derived from the production of table olives, where  
60 tyrosol and hydroxytyrosol stand out by their high concentration (Fendri et al., 2013).

61 However, despite the beneficial effect for human health, the reducing power of phenolic  
62 compounds implies a huge environmental impact if these products are directly discharged to  
63 the medium. Even at low concentrations, phenolic compounds are able to negatively impact the  
64 viability of microorganisms, plants and small vertebrates (Babic et al., 2019; Pinho et al., 2017).  
65 For these reasons, the treatment of olive mill wastewaters before their discharge to the  
66 environment is mandatory, in order to reduce the high content in organic matter and the  
67 presence of phenolic compounds, which could damage the normal plant growth and the aquatic  
68 ecosystem (Dermeche et al., 2013).

69 In consequence, the recovery of phenolic compounds from OMWW results in a reduction of the  
70 toxicity of these streams (improving their further applicability as fertilizers, compost etc) as well  
71 as a corresponding collection of high-added value products with commercial or pharmaceutical  
72 applications. In this context, membrane technology appears as a relevant approach. In the  
73 recent years, the application of membrane processes to separate bioactive compounds has  
74 emerged as a satisfactory strategy (Castro-Muñoz and Fíla, 2018). The low requirements of  
75 energy, the environmental safety, the high selectivity and the easy scale up of the process make

---

<sup>1</sup> Abbreviations used: COD: chemical oxygen demand, KSM: Kedem-Spiegler model, MWCO: molecular weight cut-off; OMWW: olive mil wastewater, TMP: transmembrane pressure.

76 membrane technology very appropriate to selectively separate and purify phenolic compounds  
77 from the rest of species present in these by-products. To achieve this objective, some aspects  
78 regarding the membrane of choice and the sample to be treated should be considered. The  
79 efficiency of the process will highly depend on the proper choice of the membrane material,  
80 interactions among the solutes present in the feed solution and the applied operational  
81 parameters (Díaz-Montes and Castro-Muñoz, 2019).

82 Also, the combination of different techniques and membrane procedures may be of interest.  
83 Some reported approaches to recover and purify phenolic compounds from OMWW are based  
84 in sequential membrane processes. For instance, Cassano and co-workers designed a process  
85 based on two ultrafiltration procedures followed by a nanofiltration step to fractionate OMWW  
86 from the three-phase olive oil production process (Cassano et al., 2013). In other cases,  
87 nanofiltration was carried out after one ultrafiltration operation (Alfano et al., 2018), or even  
88 after a microfiltration process, obtaining satisfying results in terms of COD rejection and  
89 recovery of polyphenols as well (Bazzarelli et al., 2016; Garcia-Castello et al., 2010).

90 The ultrafiltration of OMWW allows the removal of suspended solids and organic compounds of  
91 relatively high molecular weight. The corresponding permeate stream that is obtained is rich in  
92 phenolic compounds, as demonstrated by Carbonell-Alcaina et al. when wastewaters from the  
93 production of table olives were treated (Carbonell-Alcaina et al., 2018). However, a subsequent  
94 nanofiltration step is essential to remove other species of lower molecular weight that remain  
95 in the ultrafiltration permeate. Enlarging the purity of the phenolic extract highly benefits its  
96 further applicability in the industry, as they may be incorporated in cosmetic preparations, food  
97 supplements etc.

98 In this work, the viability of nanofiltration to recover tyrosol from OMWW has been investigated  
99 using as feed a model solution composed of tyrosol and sucrose. The effect of the operating  
100 conditions on the recovery has been considered. Tyrosol was selected as it is a major constituent  
101 of OMWW and it has been widely accepted as one of the principal representatives of phenolic  
102 compounds from olive-derived matrices (Borja et al., 1996; Cassano et al., 2011; Najjar et al.,  
103 2007; Richard and Delgado-Nuñez, 2003). Additionally, low molecular weight phenolic  
104 compounds have been reported to have greater antioxidant activity than polymeric ones (Syed  
105 et al., 2017). Thus, this phenolic compound attracts special interest for the cosmetic and  
106 pharmaceutical industries (Miralles et al., 2014), being its recovery a great opportunity to  
107 revalue the residues from olive mills. In the case of sucrose, it was chosen as representative of  
108 the sugars present in OMWWs.

109 The molecular weights of tyrosol ( $138.18 \text{ g} \cdot \text{mol}^{-1}$ ) and sucrose ( $342.30 \text{ g} \cdot \text{mol}^{-1}$ ) are quite similar,  
110 which hinder a proper purification of the phenolic extract. Kontos and co-workers specifically  
111 targeted the separation of tyrosol and sucrose from a synthetic solution, but it was not through  
112 a membrane process, but a cooling crystallization treatment (Kontos et al., 2018). In fact, there  
113 are not many papers addressing the partition of these two compounds and, to our knowledge,  
114 their separation by membrane processes has not been tackled in the literature despite its  
115 interest.

## 116 **1. Materials and Methods**

### 117 **1.1. Feed solutions**

118 Simulated feed solutions were prepared trying to obtain a concentration of phenolic compounds  
119 and COD similar to the actual content of real olive mill wastewaters. An olive vegetation  
120 wastewater whose characterization was previously published (Ochando-Pulido et al., 2012) was  
121 simulated. Two synthetic OMWWs were prepared: one of them only contained tyrosol (OMWW  
122 I); the second solution reproduced more accurately the actual content of OMWW, containing  
123 both tyrosol and sucrose (OMWW II). The sucrose content was the only difference between both  
124 solutions. Thus, it was possible to compare the behaviour of tyrosol by itself and that for tyrosol  
125 in the presence of the sugar. The influence of sucrose in the results and the study of its  
126 separation from the phenolic alcohol were then investigated.

127 According to the reference sample, the concentration of tyrosol (Maybridge, United Kingdom)  
128 was near to  $373 \text{ mg} \cdot \text{L}^{-1}$  for both OMWW I and OMWW II. The COD of the OMWW II was required  
129 to be  $2.875 \text{ g}$  of oxygen  $\cdot \text{L}^{-1}$ , which corresponded to a concentration of  $2.61 \text{ g} \cdot \text{L}^{-1}$  of sucrose  
130 (Panreac, Spain). Chlorhydric acid, supplied by J.T. Baker (The Netherlands) was employed to  
131 adjust the pH to 5.3, which is the typical pH of OMWW.

### 132 **1.2. Nanofiltration plant and experimental procedure**

133 To conduct the nanofiltration tests, a pilot plant was designed. It has been schematized in Figure  
134 1. The utilized feed tank had a capacity of 10 L. A NF270 membrane (Dow Chemical, EEUU), with  
135 an active area of  $0.00472 \text{ m}^2$ , was located in a flat module, which was preceded by a plunger  
136 pump. Some specifications about the membrane can be found in Table 1. Considering the  
137 molecular weight of the target molecule (tyrosol) and that of sucrose, the MWCO of the  
138 membrane was judged adequate to separate it from sucrose. A flowmeter and two manometers  
139 were employed. Each manometer was situated at the inlet and outlet side of the membrane  
140 module. The permeate stream was collected in a recipient placed onto a balance (PKP Balance,

141 Kern & Sohn GmbH, Germany) which measured the permeate mass every 5 seconds. The plant  
142 was operated in a total recycle mode; therefore, the collected permeate was periodically flowed  
143 back to the feed tank and the retentate stream was continuously recycled back to the feed tank.  
144 Temperature was controlled by means of an electric resistance, that allowed the heating of the  
145 feed solution, and a cooling coil to refrigerate it.

146 Before the conduction of any experiment, the NF membrane was washed with osmotized water  
147 (with a conductivity of  $6.5 \mu\text{S}\cdot\text{m}^{-1}$ ) to remove the preservative agent. After that, the membrane  
148 was immersed in an osmotized-water bath during 24 h, in order to hydrate it and remove  
149 impurities that might reduce its functionality. The compactation of the membrane was  
150 addressed afterwards. To this end, osmotized water was nanofiltrated during 4h, at 1 m/s and  
151 18 bar. This pressure was higher than the largest pressure applied during the experiments (15  
152 bar), to ensure that the membrane is adapted and resists this value.

153 Before the filtration experiments, pure water flux was measured at a crossflow velocity of  $1 \text{ m}\cdot\text{s}^{-1}$   
154 and different transmembrane pressures (5, 10 and 15 bar) with osmotized water in order to  
155 determine the hydraulic permeability of the membrane ( $L_p$ ) ( $L \cdot h^{-1} \cdot m^{-2} \cdot bar^{-1}$ ), according  
156 to the following equation:

$$157 \quad L_p = \frac{J_p}{\Delta P} \quad (1)$$

158 where  $J_p$  ( $L \cdot h^{-1} \cdot m^{-2}$ ) is the permeate flux and  $\Delta P$  ( $bar$ ) is the transmembrane pressure.

159 The simulated OMWWs were nanofiltered at different transmembrane pressures (5, 10 and 15  
160 bar) and cross-flow velocities of 0.5, 1 and  $1.5 \text{ m}\cdot\text{s}^{-1}$  until stable permeate flux and retention  
161 values were reached (1 hour). Temperature was maintained at  $25 \text{ }^\circ\text{C}$ .

162 The tested values of cross-flow velocity were decided after performing a nanofiltration  
163 experiment with type II simulated OMWW at a wide range of cross-flow velocities (0.25, 0.5,  
164 0.75, 1, 1.25 and  $1.5 \text{ m}\cdot\text{s}^{-1}$ ) and a TMP of 15 bar, as that is the tested TMP that was expected to  
165 cause the greatest membrane fouling. The indicated values of 0.5, 1 and  $1.5 \text{ m}\cdot\text{s}^{-1}$  were selected  
166 as appropriate for the subsequent experiments.

167 The membrane was conveniently cleaned after each run by flushing the pilot plant with different  
168 solutions at  $1 \text{ m}\cdot\text{s}^{-1}$ . First, tap water was flushed through the system without recirculation for 10  
169 min. Then, P3 Ultrasil 115 (Ecolab, Barcelona, Spain) was used to remove the solutes adsorbed  
170 on the membrane surface and embedded inside the membrane pores. Six litres of an aqueous  
171 solution of this detergent at pH 11 were recirculated for 1 h. Finally, the membrane was rinsed

172 with tap water (10 min, without recirculation) and then with osmotized water (5 min, without  
173 recirculation and pressure, and then at 1 bar for 30 min). Water permeability was again  
174 determined after each cleaning cycle, in order to corroborate that the membrane cleaning was  
175 efficient. The cleaning process was repeated if needed until at least a 90% of the initial  
176 membrane permeability was recovered.

### 177 1.3. Streams characterization

178 The synthetic solutions were characterized in order to measure the concentration of phenolic  
179 compounds and the COD. Moreover, 20 mL aliquots of the permeate streams were taken at  
180 time-points of 10, 30 and 55 minutes, in order to characterize them and evaluate the rejection  
181 of the solutes and the efficiency of the process to separate them. The Folin-Ciocalteu method  
182 was conducted to determine the concentration of total phenolic compounds (Singleton et al.,  
183 1999). The COD ( $\text{mg} \cdot \text{L}^{-1}$ ) was measured by means of the LCK 014 kits supplied by Hach Lange  
184 (Germany). Then, rejection ( $R$ ) of the membrane towards tyrosol or COD was calculated as:

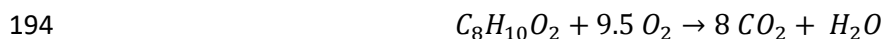
$$185 \quad R = \left(1 - \frac{C_p}{C_f}\right) \cdot 100 \quad (2)$$

186 where  $C_p$  ( $\text{mg} \cdot \text{L}^{-1}$ ) and  $C_f$  ( $\text{mg} \cdot \text{L}^{-1}$ ) are the solute concentration in the permeate and feed  
187 solution, respectively.

188 In order to estimate the percentage of the COD that corresponded only to the oxidation of  
189 tyrosol ( $COD_{TY}$ ), the following calculation was performed:

$$190 \quad COD_{TY} = \frac{TPC \cdot COD_{TY}^+}{COD} \cdot 100 \quad (3)$$

191  $TPC$  ( $\text{mg} \cdot \text{L}^{-1}$ ) corresponds to the value of total phenolic content.  $COD_{TY}^+$  ( $\text{mg oxygen} \cdot \text{mg tyrosol}^{-1}$ )  
192 is the theoretical consumption of oxygen that is necessary to oxidize one gram of tyrosol, and  
193 that is given by the chemical formula of the molecule:



195 Those 9.5 mol of oxygen that are needed to oxidize one mol of tyrosol correspond to 2.20 grams  
196 of oxygen per gram of tyrosol, which is the value of  $COD_{TY}^+$ .

### 197 1.4. Kedem-Spiegler Model



198 In order to theoretically predict the values of permeate flux obtained for the type II model  
 199 solution, which is more similar to a real OMWW, the KSM was applied (Spiegler and Kedem,  
 200 1966):

$$201 \quad J_w = J_p = L_p \cdot (\Delta P - \sigma \Delta \pi) \quad (4)$$

202 being  $\Delta \pi$  (bar) the osmotic pressure and  $\sigma$  the reflection coefficient, which is the maximal  
 203 retention that is possible for a given solute (Van der Bruggen, 2018).

204 The concentration of tyrosol was much lower than that of sucrose. Moreover, as the molecular  
 205 weight of tyrosol is lower than that of sucrose, it was expected that its rejection was lower too.  
 206 Therefore, taking into account both aspects, it can be considered that the osmotic pressure  
 207 gradient is mainly due to sucrose. On the other hand, considering that the MWCO of the  
 208 membrane is 300 Da (López-Muñoz et al., 2009) and the molecular weight of sucrose, it was  
 209 supposed that sucrose did not cross the membrane, being the reflection coefficient,  $\sigma$ , equal to  
 210 1. As a consequence, according to the KSM, the water flux ( $J_w$ ) can be defined as follows:

$$211 \quad J_w = J_p = L_p \cdot (\Delta P - \Delta \pi) \quad (5)$$

212 The osmotic pressure of a sucrose solution was determined according to the following  
 213 expression (Nabetani et al., 1992):

$$214 \quad \Delta \pi = -\frac{R_g \cdot T}{V_w} \cdot \ln \left( \frac{\frac{100 - C_m}{M_w} - \frac{4 \cdot C_m}{M_s}}{\frac{100 - C_m}{M_w} - \frac{3 \cdot C_m}{M_s}} \right) \quad (6)$$

215 where  $R_g$  ( $\text{J mol}^{-1} \text{K}^{-1}$ ) is the ideal gas constant,  $T$  is the solution temperature (K),  $V_w$  is the partial  
 216 molar volume of water (it was assumed as the partial molar volume for pure water, which is  
 217  $18.07 \cdot 10^6 \text{ m}^3 \cdot \text{mol}^{-1}$ ),  $C_m$  ( $\text{kg} \cdot \text{m}^{-3}$ ) is the concentration of sucrose on the membrane surface and  
 218  $M_s$  ( $\text{kg} \cdot \text{mol}^{-1}$ ) and  $M_w$  ( $\text{kg} \cdot \text{mol}^{-1}$ ) are the molecular weight of sucrose and water, respectively.

219  $C_m$  was calculated according to the film theory, which defines  $J_w$  as:

$$220 \quad J_w = k \cdot \ln \left( \frac{C_m - C_p}{C_f - C_p} \right) \quad (7)$$

221 In this expression,  $k$  ( $\text{m} \cdot \text{s}^{-1}$ ) is the mass transfer coefficient and  $C_f$  and  $C_p$  are solute  
 222 concentrations in the feed and in the permeate, respectively. When considering that sucrose  
 223 does not cross the membrane,  $C_p \approx 0$  and then

$$224 \quad C_m = C_f \cdot e^{\frac{J_w}{k}} \quad (8)$$

225  $k$  was determined by means of semiempirical correlations of dimensionless numbers that were  
 226 particularized for spacer-filled flat sheet and spiral wound membrane modules at turbulent flow  
 227 conditions (Schock and Miquel, 1987):

$$228 \quad Sh = 0.065 \cdot Re^{0.875} \cdot Sc^{0.25} \quad (9)$$

229 The Sherwood number ( $Sh$ ) is a function of  $k$ , the hydraulic diameter of the membrane ( $d_h$ ) (m)  
 230 and the diffusion coefficient ( $D_{AB}$ ) ( $m^2 \cdot s^{-1}$ ):

$$231 \quad Sh = \frac{k \cdot d_h}{D_{AB}} \quad (10)$$

232 The Reynolds number ( $Re$ ) is defined as function of the density of the solution ( $\rho$ ) ( $kg \cdot m^{-3}$ ), the  
 233 cross flow velocity ( $u$ ) ( $m \cdot s^{-1}$ ),  $d_h$  and the viscosity ( $\mu$ ) ( $Pa \cdot s$ ):

$$234 \quad Re = \frac{\rho \cdot u \cdot d_h}{\mu} \quad (11)$$

235 And finally, the Schmidt number ( $Sc$ ) is defined as function of  $\mu$ ,  $\rho$  and  $D_{AB}$ :

$$236 \quad Sc = \frac{\mu}{\rho \cdot D_{AB}} \quad (12)$$

237 Grouping the expressions (8, 9 and 10), the following equation is obtained:

$$238 \quad k = 0.065 \cdot \rho^{0.625} \cdot \mu^{-0.625} \cdot D_{AB}^{0.75} \cdot d_h^{-0.125} \cdot \mu^{0.875} \quad (13)$$

239 The parameters  $\rho$ ,  $\mu$  and  $D_{AB}$  were determined as previously reported (Nabetani et al., 1992),  
 240 using empirical equations. The equation to determine  $\rho$  was the following:

$$241 \quad \rho = \frac{100}{\frac{100 - C_f}{\rho_w} + \bar{v} \cdot C_f} \quad (14)$$

242 where  $\rho_w$  is the water density and  $\bar{v}$  ( $kg \cdot m^{-3}$ ) is the partial specific volume of sucrose.

243 Viscosity was calculated by the following expression, where  $\mu_w$  corresponds to water viscosity.

$$244 \quad \mu = \mu_w \cdot e^{\frac{2.61 \cdot C_f}{100 - C_f}} \quad (15)$$

245 Finally, the diffusion coefficient was determined as follows:

$$246 \quad D_{AB, in \text{ mix}} = D_{0,s} \cdot \left( \frac{\mu_w}{\mu} \right)^{0.45} \quad (16)$$

247 being  $D_{0,s}$  the diffusion coefficient of a diluted solution of sucrose ( $5.24 \cdot 10^{-10} m^2 \cdot s^{-1}$ ).

248 Taking into account all these correlations (equations 9 to 16), the simultaneous resolution of  
249 equations 5 (KSM) and 8 (film theory) allow the estimation of the concentration on the  
250 membrane surface and the permeate flux.

## 251 **2. Results and Discussion**

### 252 **2.1. Characterization of the feed solutions**

253 The synthetic OMWWs were characterized right before the nanofiltration experiments, in order  
254 to know the real concentration of the analytes, COD and pH. The obtained results can be  
255 reviewed in Table 2.

### 256 **2.2. Membrane characterization**

257 The water permeability of the membrane was determined to be  $15.73 \text{ L}\cdot\text{h}^{-1}\cdot\text{m}^{-2}\cdot\text{bar}^{-1}$ . This value  
258 was the resulting slope of the linear fitting when permeate flux was expressed as a function of  
259 TMP. The value of permeability obtained is similar to those obtained by other authors for this  
260 membrane (Avram et al., 2017).

### 261 **2.3. Variation of permeate flux with cross-flow velocity and transmembrane pressure**

262 In Figure 2, the variation of permeate flux with the cross-flow velocity for the type II model  
263 solution at a TMP of 15 bar is presented. A wide range of cross-flow velocities was contemplated.  
264 In the figure, the results of permeate flux are presented in different colours and shapes for each  
265 of the tested velocities. It can be noted that permeate flux increased with the cross-flow velocity  
266 within the considered range. However, the differences observed were not remarkable, thus  
267 indicating that concentration polarization and fouling were not severe. From these results, it  
268 was decided to continue the following set of experiments at the highest cross-flow velocity  
269 tested ( $1.5 \text{ m}\cdot\text{s}^{-1}$ ) and at two cross-flow velocities within the tested range (1 and  $0.5 \text{ m}\cdot\text{s}^{-1}$ ).

270 Figure 3 shows the obtained results for the nanofiltration of the two simulated OMWWs at the  
271 tested conditions of TMP and cross-flow velocity. Experiments conducted at the same cross-flow  
272 velocity have been plotted in the same graphic, in order to facilitate the interpretation and  
273 comparison of the results. The three graphics reflect a substantial increment of permeate flux  
274 as TMP increases. Moreover, no noticeable decline of permeate flux with time was appreciated  
275 and the values of the relative flux (compared to the flux obtained during the nanofiltration of  
276 pure water) were always above 77%, even in the case of the lowest cross-flow velocity tested.  
277 These aspects indicate that membrane fouling was not significant.

278 At 5 and 10 bar, the values of the permeate flux were very similar for both types of solutions, I  
279 and II, for all the cross-flow velocities tested. Considering the composition of each simulated  
280 solution, some differences in the values of the permeate flux could be expected. However, this  
281 variation was probably reduced because, at those TMPs, the concentration polarization  
282 phenomenon was not relevant. On the contrary, at 15 bar, the simulated solution II showed  
283 lower values of permeate flux than those observed for the solution I (only containing tyrosol).  
284 The relative flux of OMWW II ranged between 89-98% (depending on the cross-flow velocity  
285 applied), whereas OMWW I presented a relative flux of 99-100%. The higher pressure applied in  
286 this case contributed to the concentration polarization phenomenon, which was logically more  
287 significant for the simulated solution II. Similar conclusions can be reached from Figure 4, which  
288 contains the stationary permeate flux observed at every pressure and cross-flow velocity  
289 studied. The values of permeability for the three tested feeds (deionized water, OMWW I and  
290 OMWW II) were very similar, being that of deionized water greater. However, at 15 bar, the  
291 lower permeate flux of OMWW II was more noticeable. It can also be observed that as cossflow  
292 velocity increases, the difference between the permeability for OMWW I and OMWW II  
293 decreases.

#### 294 **2.4. Rejection of solutes**

295 The just discussed difference in the values of permeate flux observed at 15 bar occurred mainly  
296 at the cross-flow velocities of 0.5 and 1 m·s<sup>-1</sup>. However, at 1.5 m·s<sup>-1</sup> the values of permeate flux  
297 for both solutions were much closer. Higher values of cross-flow velocity provided a major  
298 turbulence inside the membrane module that contributed to the back diffusion of solute from  
299 the membrane surface, thus reducing the concentration polarization phenomenon, featuring  
300 higher values of permeate flux when compared with lower velocities. The highest influence of  
301 cross-flow velocity on permeate flux was observed at the largest TPM tested (15 bar), as at this  
302 TMP the convective transport of solutes towards the membrane is greatest and, therefore, the  
303 concentration polarization phenomenon is more significant. Figure 5A shows the rejection of  
304 phenolic compounds at different operating conditions. The data presented in the figure  
305 corresponds to steady state rejection. As it can be observed, low rejection values of tyrosol were  
306 obtained. The NF270 membrane hardly retained the phenolic compound, which facilitated its  
307 recovery in the permeate stream. In contrast, Avram and co-workers reported a complete  
308 rejection of phenolic compounds from hot water extracts of blueberry pomace, using the same  
309 membrane (Avram et al., 2017). This discrepancy is explained by the MWCO of the membrane  
310 and the substantial difference between the molecular weight of tyrosol (present in the  
311 simulated OMWWs) and the large-size polyphenols from the blueberry pomace (mainly

312 anthocyanins). Also, some polymerizations may have occurred among the molecules of the  
313 extract, thus increasing the rejection. In our case, the molecular weight of tyrosol was  
314 considered and the membrane NF270 was carefully chosen in order not to retain the compound  
315 of interest, but to separate it from the sugar present in the feed solution. Regarding the potential  
316 electrostatic interactions between the membrane and the compound of interest, the isoelectric  
317 point of the NF270 membrane has been described to be in the range of 3.3-5.2 (Mänttari et al.,  
318 2006; Nghiem et al., 2005). Being the pH of the OMWWs around 5.3, it is reasonable to assume  
319 that the membrane surface may be negatively charged, at least partially. However, this scenario  
320 did not conflict with the permeation of tyrosol, because the molecule was neutral at the working  
321 pH, since it has been observed by several authors that pH values greater than 9 have to be  
322 reached in order to obtain tyrosol in its deprotonated form (Vulcano et al., 2015; Carrasco-  
323 Pancorbo et al., 2006). This facilitated the diffusion of tyrosol to the membrane and the  
324 subsequent low rejection that was observed.

325 According to the figure 5A, when the TMP was increased from 5 to 10 bar, rejection raised too,  
326 which is in accordance with the KSM for a nanofiltration process. However, when the TMP  
327 increased from 10 to 15 bar, phenolic compounds rejection decreased, which may be explained  
328 by a fouling phenomenon, prompted by the concentration polarization that was favoured at this  
329 pressure level. The effect of cross-flow velocity was barely observed, as the differences in  
330 rejection with the variations of the velocity were very small. Nevertheless, rejection did slightly  
331 increase with the cross-flow velocity, as expected. As can be seen in the figure, phenolic  
332 compounds rejections for the simulated OMWW II were lower than those for the solution I. This  
333 effect was not related with a reduction in the permeate flux, as could be expected (Bellona et  
334 al., 2004), because, according to Figure 3 and Figure 4, the values of permeate flux were similar  
335 for both types of simulated solutions. As explained before, the fouling of the membrane was not  
336 harsh, thus, the observed values of permeate flux were very similar for both solutions. Instead,  
337 the decrease in the rejection for the simulated solution II may be explained by an increase in the  
338 viscosity of OMWW II (prompted by the presence of sucrose). In that case, the mass transfer  
339 coefficient of tyrosol,  $k$ , would be affected too. This parameter is a diffusion rate constant  
340 related to the back diffusion of tyrosol from the membrane surface towards the bulk solution. If  
341  $k$  is lower, the concentration of tyrosol on the membrane surface,  $C_m$ , is higher, which results in  
342 an increase of the concentration in the permeate and the subsequent decrease of the rejection.

343 Additionally, Figure 6 shows the values of rejection obtained at the different operation times. In  
344 general, the rejection values observed for a given pressure and cross-flow velocity scarcely  
345 varied with time, which confirms that the occurring fouling of the membrane was low. However,

346 at the highest TMP tested (15 bar), the rejection slightly increased with time, what indicates that  
347 fouling is more noticeable at this TMP.

348 COD rejection for both simulated solutions at the different operating conditions that were  
349 tested is shown in Figure 5B. The data refer to steady state rejection. The same as it was  
350 observed for the rejection of phenolic compounds, the differences of COD rejection observed  
351 during the time were very small. The variation of COD rejection with TMP and cross-flow velocity  
352 followed the same trend that was already commented for the phenolic compounds.  
353 Nevertheless, the simulated OMWW II displayed much higher COD rejections than the simulated  
354 OMWW I, what indicates that sucrose rejection was very high, as sucrose is only present in  
355 OMWW II and not in OMWW I. As tyrosol rejection was observed to be low and sucrose is the  
356 only additional component in OMWW II, it is assumable that sucrose was being rejected in a  
357 high percentage. These rejection values were indicative of the selectivity of the process, which  
358 led to a permeate stream enriched in tyrosol and purified from the rest of components of  
359 the feed solution. Indeed, the percentage of COD in the permeate stream that corresponded  
360 only to tyrosol (calculated according to equation 3), which is shown in Figure 7, was above 90%  
361 for all the operating conditions tested. This indicated that practically the whole organic matter  
362 that was present in the permeate was tyrosol itself. The initial objective of the study (based on  
363 the separation of tyrosol from the sugars of the OMWW) was then satisfactorily achieved. On  
364 the other hand, the assumption of a value of  $\sigma$  equal to 1 for sucrose that was made at the  
365 beginning to predict the values of the permeate flux was confirmed to be correct.

366 According to these results, a TMP of 15 bar and a cross-flow velocity of  $0.5 \text{ m}\cdot\text{s}^{-1}$  were selected  
367 as optimum for the separation of tyrosol and sucrose. The observed fouling was considered  
368 minor, whereas the highest permeate flux (above  $225 \text{ L}\cdot\text{h}^{-1}\cdot\text{m}^{-2}$ ) (Figure 3) and the lowest  
369 phenolic compounds rejection were obtained ( $12.3\% \pm 0.2\%$ , for OMWW II) (Figure 5). All these  
370 parameters should be further studied with real OMWW. Ongoing experiments are being  
371 conducted in our lab in this regard. In any case, at these conditions, it is possible to obtain a pure  
372 product, perfectly able to be incorporated in other preparations, as cosmetic or nutraceutical  
373 formulas. The format of the final product will determine if more treatments are needed, as  
374 drying, encapsulation etc. However, as the tyrosol is recovered in an aqueous phase, the solution  
375 is biocompatible, safe and easy to handle.

## 376 **2.5. Predictions of Kedem-Spiegler Model**

377 KSM was initially conceived for reverse osmosis operations; nevertheless, it has been  
378 successfully applied to the nanofiltration of uncharged molecules in previous reports (Cuartas-

379 Uribe et al., 2010, 2007). The values of different parameters estimated by means of the  
380 combination of the KSM and the film theory for the solution II are listed in Table 3. This Table  
381 also contains the calculated Reynolds numbers, according to equation 11. All values of Re were  
382 above 1000. Schock and Miquel demonstrated that Re values above 400 correspond to turbulent  
383 flow when working with spacer-filled spiral wound or flat sheet elements (Schock and Miquel,  
384 1987). This conclusion supports the application of equation 9.

385 To facilitate the comparison with the experimental results, only one value of experimental  
386 permeate flux has been given. This is the media of each registered value after 30 minutes of  
387 operation, where the steady state was achieved and the flux was constant. The table reflects  
388 the phenomenon that has been commented in the previous sections: an increase in the cross-  
389 flow velocity is related with an increase in the turbulence inside the membrane module, which  
390 contributes to increase the back-diffusion of the solute towards the bulk solution and produces  
391 a decline in the osmotic pressure gradient due to the lower concentration of sucrose on the  
392 membrane surface. The theoretical values of permeate flux predicted by the model were  
393 accurately confirmed by the experimental values. According to Figure 8, good agreement was  
394 achieved. The difference between estimated and experimental data was lower than 5% in all  
395 cases (Table 3).

396 The values of  $J_p$  experimentally observed were lower than the predicted ones, as a consequence  
397 of membrane fouling, which is not contemplated by the KSM and causes the corresponding  
398 resistance to the permeation through the membrane (Giacobbo et al., 2018). As the  
399 discrepancies between experimental and theoretical flux were very small, membrane fouling  
400 can be considered to be small too. Additionally, differences between predicted and  
401 experimental values of permeate flux can be also justified by the small fraction of sucrose that  
402 was not retained by the membrane. The consideration of  $\sigma$  equal to 1 was indeed reasonable,  
403 but, as the sucrose rejection did not achieved the 100%, it could contribute to some  
404 discrepancies between the model and the experimental results.

### 405 **3. Conclusions**

406 An efficient nanofiltration process to purify phenolic compounds from OMWWs has been  
407 developed. Special attention has been given to their separation from sugars due to the similar  
408 molecular weight. The increase of TMP resulted in higher permeate fluxes. Similarly, higher  
409 values of cross-flow velocity contributed to remove the solutes from the membrane surface and  
410 reduce the concentration polarization effect.

411 Tyrosol was observed to be recovered in the permeate stream, as the values of rejection ranged  
412 between  $12.3\% \pm 0.2\%$  and  $23.9\% \pm 0.7\%$ . COD rejection ranged between 77.8% and 83.9%. From  
413 the low values of COD that were determined in the permeate, more than 90% of the permeate  
414 COD can be attributed to tyrosol. Thus, it can be concluded that sucrose was highly retained by  
415 the membrane. Rejection to both tyrosol and COD increased with the increment of TMP and  
416 cross-flow velocity, but the effect of TMP was more significative.

417 The obtained values of permeate flux were accurately predicted by the KSM. The error was  
418 always under 4.7%, which demonstrates that the KSM was an appropriate model to predict the  
419 effect of the operating conditions on the permeate flux.

420 The results presented here demonstrate the suitability of membrane technology and,  
421 specifically, nanofiltration, to recover valued bioactive compounds from olive mill wastes. The  
422 retirement of the phenolic compounds from the by-products generated during the olive oil  
423 campaign contributes to their decontamination and also constitutes their revalorization,  
424 through the future industrialization of the obtained beneficial molecules.

#### 425 **Acknowledgements**

426 This work was supported by the Spanish Ministry of Economy, Industry and Competitiveness  
427 through the project CTM2017-88645-R, and by the Spanish Ministry of Science, Innovation and  
428 Universities through the PRE2018-085245 pre-doctoral grant.

429

#### 430 **References**

- 431 Alfano, A., Corsuto, L., Finamore, R., Savarese, M., Ferrara, F., Falco, S., Santabarbara, G., De  
432 Rosa, M., Schiraldi, C., 2018. Valorization of olive mill wastewater by membrane  
433 processes to recover natural antioxidant compounds for cosmeceutical and nutraceutical  
434 applications or functional foods. *Antioxidants* 7. <https://doi.org/10.3390/antiox7060072>
- 435 Avram, A.M., Morin, P., Brownmiller, C., Howard, L.R., Sengupta, A., Wickramasinghe, S.R.,  
436 2017. Concentrations of polyphenols from blueberry pomace extract using nanofiltration.  
437 *Food Bioprod. Process.* 106, 91–101. <https://doi.org/10.1016/j.fbp.2017.07.006>
- 438 Babic, S., Malev, O., Maryline, P., Lebedev, A.T., Mazur, D.M., Ku, A., Rozelindra, Č., Treb, P.,  
439 2019. Toxicity evaluation of olive oil mill wastewater and its polar fraction using multiple  
440 whole-organism bioassays. *Sci. Total Environ.* 686, 903–914.  
441 <https://doi.org/10.1016/j.scitotenv.2019.06.046>



442 Bazzarelli, F., Piacentini, E., Poerio, T., Mazzei, R., Cassano, A., Giorno, L., 2016. Advances in  
443 membrane operations for water purification and biophenols recovery/valorization from  
444 OMWWs. *J. Memb. Sci.* 497, 402–409. <https://doi.org/10.1016/j.memsci.2015.09.049>

445 Bellona, C., Drewes, J.E., Xu, P., Amy, G., 2004. Factors affecting the rejection of organic solutes  
446 during NF/RO treatment - A literature review. *Water Res.* 38, 2795–2809.  
447 <https://doi.org/10.1016/j.watres.2004.03.034>

448 Borja, R., Banks, C.J., Maestro-Durán, R., Alba, J., 1996. The effects of the most important  
449 phenolic constituents of olive mill wastewater on batch anaerobic methanogenesis.  
450 *Environ. Technol. (United Kingdom)* 17, 167–174.  
451 <https://doi.org/10.1080/09593331708616373>

452 Carbonell-Alcaina, C., Álvarez-Blanco, S., Bes-Piá, M.A., Mendoza-Roca, J.A., Pastor-Alcañiz, L.,  
453 2018. Ultrafiltration of residual fermentation brines from the production of table olives at  
454 different operating conditions. *J. Clean. Prod.* 189, 662–672.  
455 <https://doi.org/10.1016/j.jclepro.2018.04.127>

456 Carrasco-Pancorbo, A., Gómez-Caravaca, A.M., Cerretani, L., Bendini, A., Segura-Carretero, A.,  
457 Fernández-Gutiérrez, A., 2006. Rapid Quantification of the Phenolic Fraction of Spanish  
458 Virgin Olive Oils by Capillary Electrophoresis with UV Detection, *J. Agric. Food Chem.*,  
459 54(21), 7984–7991

460 Casaburi, I., Puoci, F., Chimento, A., Sirianni, R., Ruggiero, C., Avena, P., Pezzi, V., 2013.  
461 Potential of olive oil phenols as chemopreventive and therapeutic agents against cancer:  
462 A review of in vitro studies. *Mol. Nutr. Food Res.* 57, 71–83.  
463 <https://doi.org/10.1002/mnfr.201200503>

464 Cassano, A., Conidi, C., Drioli, E., 2011. Comparison of the performance of UF membranes in  
465 olive mill wastewaters treatment. *Water Res.* 45, 3197–3204.  
466 <https://doi.org/10.1016/j.watres.2011.03.041>

467 Cassano, A., Conidi, C., Giorno, L., Drioli, E., 2013. Fractionation of olive mill wastewaters by  
468 membrane separation techniques. *J. Hazard. Mater.* 248–249, 185–193.  
469 <https://doi.org/10.1016/j.jhazmat.2013.01.006>

470 Castro-Muñoz, R., Fíla, V., 2018. Membrane-based technologies as an emerging tool for  
471 separating high-added-value compounds from natural products. *Trends Food Sci.*  
472 *Technol.* <https://doi.org/10.1016/j.tifs.2018.09.017>

473 Cuartas-Uribe, B., Vincent-Vela, M.C., Álvarez-Blanco, S., Alcaina-Miranda, M.I., Soriano-Costa,  
474 E., 2010. Application of nanofiltration models for the prediction of lactose retention using  
475 three modes of operation. *J. Food Eng.* 99, 373–376.  
476 <https://doi.org/10.1016/j.jfoodeng.2010.03.023>

477 Cuartas-Uribe, B., Vincent-Vela, M.C., Álvarez-Blanco, S., Alcaina-Miranda, M.I., Soriano-Costa,  
478 E., 2007. Nanofiltration of sweet whey and prediction of lactose retention as a function of  
479 permeate flux using the Kedem-Spiegler and Donnan Steric Partitioning models. *Sep. Purif.*  
480 *Technol.* 56, 38–46. <https://doi.org/10.1016/j.seppur.2007.01.006>

481 Dermeche, S., Nadour, M., Larroche, C., Moulti-Mati, F., Michaud, P., 2013. Olive mill wastes:  
482 Biochemical characterizations and valorization strategies. *Process Biochem.* 48, 1532–  
483 1552. <https://doi.org/10.1016/j.procbio.2013.07.010>

484 Di Mauro, M.D., Giardina, R.C., Fava, G., Mirabella, E.F., Acquaviva, R., Renis, M., D’Antona, N.,  
485 2017. Polyphenolic profile and antioxidant activity of olive mill wastewater from two  
486 Sicilian olive cultivars: Cerasuola and Nocellara etnea. *Eur. Food Res. Technol.* 243, 1895–  
487 1903. <https://doi.org/10.1007/s00217-017-2893-3>

488 Díaz-Montes, E., Castro-Muñoz, R., 2019. Metabolites recovery from fermentation broths via  
489 pressure-driven membrane processes. *Asia-Pacific J. Chem. Eng.*  
490 <https://doi.org/10.1002/apj.2332>

491 Fendri, I., Chamkha, M., Bouaziz, M., Labat, M., Sayadi, S., Abdelkafi, S., 2013. Olive  
492 fermentation brine: Biotechnological potentialities and valorization. *Environ. Technol.*  
493 (United Kingdom) 34, 183–193. <https://doi.org/10.1080/09593330.2012.689364>

494 Garcia-Castello, E., Cassano, A., Criscuoli, A., Conidi, C., Drioli, E., 2010. Recovery and  
495 concentration of polyphenols from olive mill wastewaters by integrated membrane  
496 system. *Water Res.* 44, 3883–3892. <https://doi.org/10.1016/j.watres.2010.05.005>

497 Ghanbari, R., Anwar, F., Alkharfy, K.M., Gilani, A.H., Saari, N., 2012. Valuable nutrients and  
498 functional bioactives in different parts of olive (*Olea europaea* L.)-A review, *International*  
499 *Journal of Molecular Sciences.* <https://doi.org/10.3390/ijms13033291>

500 Giacobbo, A., Bernardes, A.M., Rosa, M.J.F., De Pinho, M.N., 2018. Concentration polarization  
501 in ultrafiltration/nanofiltration for the recovery of polyphenols from winery wastewaters.  
502 *Membranes (Basel).* 8. <https://doi.org/10.3390/membranes8030046>

503 Kontos, S.S., Katrivesis, F.K., Constantinou, T.C., Zoga, C.A., Ioannou, I.S., Koutsoukos, P.G.,  
504 Paraskeva, C.A., 2018. Implementation of membrane filtration and melt crystallization for  
505 the effective treatment and valorization of olive mill wastewaters. *Sep. Purif. Technol.*  
506 193, 103–111. <https://doi.org/10.1016/j.seppur.2017.11.005>

507 López-Miranda, J., Pérez-Jiménez, F., Ros, E., De Caterina, R., Badimón, L., Covas, M.I., Escrich,  
508 E., Ordovás, J.M., Soriguer, F., Abiá, R., Alarcón de la Lastra, C., Battino, M., Corella, D.,  
509 Chamorro-Quirós, J., Delgado-Lista, J., Giugliano, D., Esposito, K., Estruch, R., Fernandez-  
510 Real, J.M., Gaforio, J.J., La Vecchia, C., Lairon, D., López-Segura, F., Mata, P., Menéndez,  
511 J.A., Muriana, F.J., Osada, J., Panagiotakos, D.B., Paniagua, J.A., Pérez-Martinez, P.,  
512 Perona, J., Peinado, M.A., Pineda-Priego, M., Poulsen, H.E., Quiles, J.L., Ramírez-Tortosa,  
513 M.C., Ruano, J., Serra-Majem, L., Solá, R., Solanas, M., Solfrizzi, V., de la Torre-Fornell, R.,  
514 Trichopoulou, A., Uceda, M., Villalba-Montoro, J.M., Villar-Ortiz, J.R., Visioli, F.,  
515 Yiannakouris, N., 2010. Olive oil and health: Summary of the II international conference  
516 on olive oil and health consensus report, Jaén and Córdoba (Spain) 2008. *Nutr. Metab.*  
517 *Cardiovasc. Dis.* 20, 284–294. <https://doi.org/10.1016/j.numecd.2009.12.007>

518 López-Muñoz, M.J., Sotto, A., Arsuaga, J.M., Van der Bruggen, B., 2009. Influence of  
519 membrane, solute and solution properties on the retention of phenolic compounds in  
520 aqueous solution by nanofiltration membranes. *Sep. Purif. Technol.* 66, 194–201.  
521 <https://doi.org/10.1016/j.seppur.2008.11.001>

522 Mänttari, M., Pihlajamäki, A., Nyström, M., 2006. Effect of pH on hydrophilicity and charge and  
523 their effect on the filtration efficiency of NF membranes at different pH. *J. Memb. Sci.*  
524 280, 311–320. <https://doi.org/10.1016/j.memsci.2006.01.034>

525 Miralles, P., Chisvert, A., Salvador, A., 2014. Determination of hydroxytyrosol and tyrosol by  
526 liquid chromatography for the quality control of cosmetic products based on olive  
527 extracts. *J. Pharm. Biomed. Anal.* 102, 157–161.  
528 <https://doi.org/10.1016/j.jpba.2014.09.016>

529 Nabetani, H., Nakajima, M., Watanabe, A., Nakao, S.I., Kimura, S., 1992. Prediction of the flux  
530 for the reverse osmosis of a solution containing sucrose and glucose. *J. Chem. Eng. Japan*  
531 25, 575–580. <https://doi.org/10.1252/jcej.25.575>

532 Najjar, W., Azabou, S., Sayadi, S., Ghorbel, A., 2007. Catalytic wet peroxide photo-oxidation of  
533 phenolic olive oil mill wastewater contaminants. Part I. Reactivity of tyrosol over (Al-  
534 Fe)PILC. *Appl. Catal. B Environ.* 74, 11–18. <https://doi.org/10.1016/j.apcatb.2007.01.007>

535 Nghiem, L.D., Schäfer, A.I., Elimelech, M., 2005. Pharmaceutical retention mechanisms by  
536 nanofiltration membranes. *Environ. Sci. Technol.* 39, 7698–7705.  
537 <https://doi.org/10.1021/es0507665>

538 Ochando-Pulido, J.M., Rodriguez-Vives, S., Hodaifa, G., Martinez-Ferez, A., 2012. Impacts of  
539 operating conditions on reverse osmosis performance of pretreated olive mill  
540 wastewater. *Water Res.* 46, 4621–4632. <https://doi.org/10.1016/j.watres.2012.06.026>

541 Olmo-García, L., Kessler, N., Neuweger, H., Wendt, K., Olmo-Peinado, J.M., Fernández-Guti  
542 rrez, A., Baessmann, C., Carrasco-Pancorbo, A., 2018. Unravelling the distribution of  
543 secondary metabolites in *olea europaea* L.: exhaustive characterization of eight olive-tree  
544 derived matrices by complementary platforms (LC-ESI/APCI-MS and GC-APCI-MS).  
545 *Molecules* 23, 1–16. <https://doi.org/10.3390/molecules23102419>

546 Pinho, A., Lopes, D. V, Martins, R.C., Quina, M.J., 2017. Phytotoxicity assessment of olive mill  
547 solid wastes and the influence of phenolic compounds. *Chemosphere* 185, 258–267.  
548 <https://doi.org/10.1016/j.chemosphere.2017.07.002>

549 Ray, N.B., Hilsabeck, K.D., Karagiannis, T.C., McCord, D.E., 2019. Bioactive Olive Oil Polyphenols  
550 in the Promotion of Health, in: *The Role of Functional Food Security in Global Health*.  
551 Elsevier Inc., pp. 623–637. <https://doi.org/10.1016/b978-0-12-813148-0.00036-0>

552 Richard, D., Delgado-Nuñez, M.D.L., 2003. Kinetics of the degradation by catalytic  
553 hydrogenation of tyrosol, a model molecule present in olive oil waste waters. *J. Chem.*  
554 *Technol. Biotechnol.* 78, 927–934. <https://doi.org/10.1002/jctb.876>

555 Schock, G., Miquel, A., 1987. Mass transfer and pressure loss in spiral wound modules.  
556 *Desalination* 64, 339–352. [https://doi.org/10.1016/0011-9164\(87\)90107-X](https://doi.org/10.1016/0011-9164(87)90107-X)

557 Singleton, V.L., Orthofer, R., Lamuela-Raventós, R.M., 1999. Analysis of total phenols and other  
558 oxidation substrates and antioxidants by means of folin-ciocalteu reagent. *Methods*  
559 *Enzymol.* 299, 152–178. [https://doi.org/10.1016/S0076-6879\(99\)99017-1](https://doi.org/10.1016/S0076-6879(99)99017-1)

560 Spiegler, K.S., Kedem, O., 1966. Thermodynamics of hyperfiltration (reverse osmosis): Criteria  
561 for efficient membranes. *Desalination* 1, 311–326.

562 Syed, U.T., Brazinha, C., Crespo, J.G., Ricardo-da-Silva, J.M., 2017. Valorisation of grape  
563 pomace: Fractionation of bioactive flavan-3-ols by membrane processing. *Sep. Purif.*  
564 *Technol.* 172, 404–414. <https://doi.org/10.1016/j.seppur.2016.07.039>

- 565 Van der Bruggen, B., 2018. Microfiltration, ultrafiltration, nanofiltration, reverse osmosis, and  
566 forward osmosis, in: Luis, P. (Ed.), *Fundamental Modelling of Membrane Systems*.  
567 Elsevier Inc., pp. 25–70. <https://doi.org/10.1016/b978-0-12-813483-2.00002-2>
- 568 Vulcano, I, Halabalaki, I, Skaltsounis, L., Ganzera, M., 2015. Quantitative analysis of pungent  
569 and anti-inflammatory phenolic compounds in olive oil by capillary electrophoresis, *Food*  
570 *Chem.* DOI: 10.1016/j.foodchem.2014.08.007